Chapter 5 Enhanced bioactivity, biocompatibility and mechanical behavior of strontium substituted bioactive glasses

5.1 Introduction

A significant challenge is posed for regeneration of large size bone defects generally caused due to infections, trauma, accidents, tumors or genetic malformations in the human body. It necessitates the need for effective materials of bone regeneration and tissue engineering capability. Multifunctional bioactive glasses offer an excellent opportunity in delivering therapeutic ions like strontium (Sr) [10,122,123], a trace element in the human body. Sr has been found to exert anabolic and anti-catabolic effects on bone metabolism. It is beneficial for biological applications, specially for the formation of healthy bone growth which stimulates the bone formation and reduces the resorption having favorable effects on osteogenesis and angiogenesis [50,53,55,56,122,124]. The amount of strontium in human bone is typically only 3.5% of its calcium content. The majority of the absorbed Sr is localized in bone, particularly at regions of high metabolic turnover [125]. Potential applications of Sr have been reported for treatment of osteoporosis and regaining of bone mass [58,89–91,126,127]. Bioactive glasses are able to form interfacial bonds with living organisms of hard and soft tissues by their degradation in physiological solutions and formation of a stable hydroxyl-carbonate apatite (HCA) layer on the glass surface [1,31]. The SiO_2–Na_2O–CaO–P_2O_5 glass system has higher bioactivity in comparison to HA [2,3]. The bioactive glass (45S5 bioglass®) has been studied extensively and is being used as bone regenerative material in orthopaedic and dental applications [1,31]. Further, It was reported that the strontium substituted bioactive glasses are superior biomaterial in

comparison to 45S5 bioglass® [48,55,88]. Hence, it authenticates that strontium being an ideal element is positive for substitution in bioactive glasses. However, many reports mentioned that substitution of SrO for CaO retards the formation of HA in simulated body fluid (SBF) and there is lack of a detailed mechanical behavior analysis of those bioglasses (BG). For treatment of large bone defects, mechanical properties need to be considered essentially [111]. A biomaterial must be able to withstand against mechanical stress caused during surgical handling and post implantation to complete HA transformation. Thus, expediting the patient's recovery and improving the clinical consequences. Network connectivity (NC) can be used to predict a number of properties, such as structural, chemical, mechanical, bioactivity and biological [25–27]. NC depicts the average number of bridging oxygen (BOs) atoms per glass forming elements in the glass structure. In general, the glass NC tends to decrease with increasing the concentration of modifiers.

It is still a challenge to develop new biomaterials which would develop HA quickly for providing adequate mechanical strength. Many research reports are available on SrO substitution for CaO in bioactive glasses [48,52–54,92,113,128]. To the best of our knowledge, the substitution of SrO for SiO_2 in a bioactive glass has never been reported earlier. The new compositions show a significant effect on the glass density and network connectivity and which will have immense effect on bioactivity, cytocompatibility and mechanical behavior. The present work systematically report the *in vitro* bioactivity and cell cultural studies (viability, cytotoxicity, proliferation, cell apoptosis and cell attachement) as well as mechanical behavior of the bioactive glasses

5.2 Materials and methods:

5.2.1 Formulation of bioactive glass composition

Four bioactive glass compositions were formulated in a five component system (Na_2O–CaO–SrO–P_2O_5–SiO_2) along with the 45S5 bioglass® was also prepared for comparison as shown in **Table 5.1**. The bioactive glass (Sr-1) was prepared as a reference samples where SrO substituted for CaO and which is very close to Donnell et al glass composition (Sr7.5) [55]. The new formulations containing partially substituted SrO for SiO_2 on the molar basis. Network Connectivity (NC) was calculated on the basis of general equation (5.1) [25,28] assuming that SiO_2 form the network structure in the glass whereas, P_2O_5 remains in orthophosphate phase.

$$NC = \frac{4 \text{ x } SiO_2 + 6 \text{ x } P_2O_5 - (2 \text{ x } CaO + 2 \text{ x } SrO + 2 \text{ x } Na_2O)}{SiO_2} \quad -(5.1)$$

5.2.2 Preparation of the bioactive glasses

The bioactive glasses shown in **Table 5.1** were prepared by melting analytical reagent grade calcined quartz (purity 99.9%), sodium carbonate (99.5%), calcium carbonate (98%), strontium carbonate (99.5%) and ammonium dihydrogen orthophosphate (99%) as a source of SiO_2, Na_2O, CaO, SrO and P_2O_5, respectively. The weighed batches were mixed for 30 minutes in an agate mortar and pestle and melted in a platinum crucible at 1400°C for 2 h in an electrical furnace. In order to ensure homogeneity, the glass melts were taken out of the furnace, poured on a preheated aluminum plate, cooled, crushed and re-melted in the furnace for an another period of 2 h. The bulk glass samples were annealed in a pre-heated furnace at 450 °C and after 1 h of annealing, the furnace was cooled to room temperature. The bulk glass samples were cut and polished into required dimensions. The polished glass samples

were ultrasonically cleaned in an acetone bath. The densities of the glasses were determined by ASTM B962-14 method. The oxygen density of the bioactive glass was calculated using equation (5.2) to measure the compactness of the glass structure according to earlier reports [48,115].

$$OD = \frac{M_O \times (2X_{SiO_2} + 5X_{P_2O_5} + X_{Na_2O} + X_{CaO} + X_{SrO})}{[M_{SiO_2}X_{SiO_2} + M_{P_2O_5}X_{P_2O_5} + M_{Na_2O}X_{Na_2O} + M_{CaO}X_{CaO} + M_{SrO}X_{SrO}] \times \rho_{exp}^{-1}} - (5.2)$$

Where OD= oxygen density; M_O is the atomic mass of oxygen; X_{SiO_2}, $X_{P_2O_5}$, X_{Na_2O}, X_{CaO} and X_{SrO} are the molar fractions of SiO_2, P_2O_5, Na_2O, CaO and SrO, respectively; M_{SiO_2}, $M_{P_2O_5}$, M_{Na_2O}, M_{CaO} and M_{SrO} are the masses of SiO_2, P_2O_5, Na_2O, CaO and SrO, respectively and ρ_{exp} is the experimental glass density.

Table 5.1 Chemical composition of the bioactive glasses (mol %).

Glass code	SiO_2	P_2O_5	CaO	Na_2O	SrO	NC
Sr-0 (45S5)	46.10	2.60	26.90	24.40	0.00	2.11
Sr-1	46.10	2.60	24.22	24.40	2.00	2.11
Sr-2	45.10	2.60	26.90	24.40	1.00	2.03
Sr-3	44.10	2.60	26.90	24.40	2.00	1.94
Sr-4	43.10	2.60	26.90	24.40	3.00	1.84

5.3 Results and Discussion:

5.3.1 Thermal behavior of glass

Figure 5.1 (A) shows the thermal behavior of the bioactive glasses (Sr-0, Sr-1, Sr-2, Sr-3 and Sr-4) with respect to temperature. The substitution of SrO for SiO_2 in the system demonstrates a significant effect on glass transition (T_g) and crystallization (T_c) temperatures and both were found to decrease from 543 (Sr-0) to 524 ^oC (Sr-4) and 687 (Sr-0) to 627 ^oC (Sr-4), respectively. The change in enthalpy is directly related to the mobility of the atoms in the glass network [129]. It was observed that, an increase in SrO content for SiO_2 in the base bioactive glass (45S5) exhibited a linear decrease of endothermic and exothermic peaks towards lower temperatures. It was depicted that an addition of modifier in the glass breaks the bonds of SiO_4 network and creates more NBOs during reheating these glasses devitrify faster [98]. Furthermore, earlier studies have shown that the substitution SrO for SiO_2 in 45S5 bioglass and in an another series of bioactive glasses caused a decrease in Tg and increase in Tc points[51,55,115,130]. Thus, an increase in sintering window ($\Delta T=Tc-Tg$). This due to the fact that the modifier was substituted by another one which did not alter the glass network connectivity greatly and this effect could be seen in Sr-1 sample. In present study, the sintering window decreases significantly with increasing the concentration of SrO for SiO_2 as shown in **Figure 5.1 (B)**. This decrease could be associated with the glass NC, which devitrify quite early [25,51]. Therefore, the substitution of SrO for SiO_2 significantly affected on glass structure.

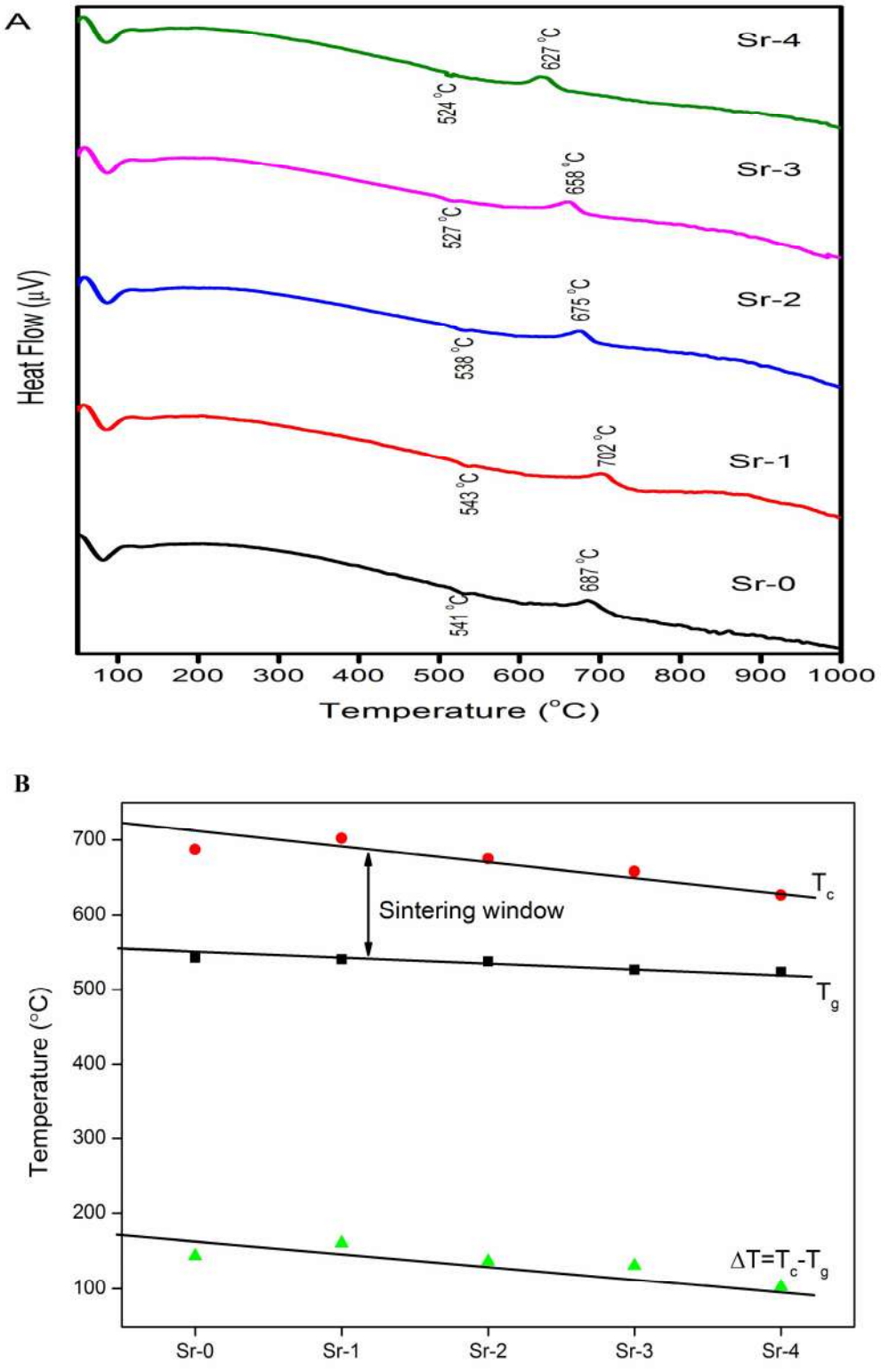

Figure 5.1 (A) DTA curves of the bioactive glass samples (Sr-0, Sr-1, Sr-2, Sr-3 and Sr-4) and (B) Glass transition, crystallization temperatures and sintering window of bioactive glasses (Sr-0, Sr-1, Sr-2, Sr-3 and Sr-4).

5.3.2 Assessment of bioactivity in SBF

A. pH Behavior of the SBF

Figure 5.2 represents the change in pH of the SBF after immersion of the samples for different time periods. The mechanism of HCA formation can be assessed by the pH behavior of SBF after immersion of the samples [1,31,131]. The pH behaviors of all the bioactive glasses show similar trends. The pH of SBF increased significantly from an initial value of 7.38 to 9.02, 8.25, 8.51, 8.72 and 8.38 for Sr-0, Sr-1, Sr-2, Sr-3 and Sr-4, respectively after 3 days of immersion. The appreciable increase in pH demonstrates the dissolution of cations from the surface of the glass. The high pH leads an attack on silica network and formation of silanols. After three days immersion, the pH of the SBF decreased in all the samples, which is due to the absorption of calcium and phosphate ions from the SBF to promote the HCA layer formation on the surface of the samples [31,132]. Fourth day onwards pH remained almost constant due to the migration of amorphous $CaO\text{-}P_2O_5$ rich film by incorporation of soluble calcium and phosphates from the solution [130]. Therefore, the results demarcate that the substitution of SrO for SiO_2 in the present investigation did not alter the bioactivity mechanism in SBF. It is interesting to discuss that Sr-0 sample attained highest pH as compared with rest of the samples on day 3. While Sr-1 has lowest pH, this decrease can be attributed to a better coupling of metal–oxygen (M–O) bond strength of Sr–O. It has been reported by Goel et al. [130] and Lao et al. [113] that the substitution of SrO for CaO in bioactive glasses minimize the dissolution kinetics due to greater M-O bond strength of strontium (351 kJ mol^{-1} and 389 kJ mol^{-1} for Ca–O and Sr–O, respectively). Thus, the ability to exchange Sr^{2+} ion with H^{+} ion decreases in SBF and hence a lower pH value was reported. This is in conformity with the present results of Sr-1.

In presence of Sr-2, Sr-3 and Sr-4 low NC bioactive glasses (low NCB glasses), the pH values were reported more than Sr-1 on day 3 which confirms release of ions from the glasses. Hence, these results suggest that the substitution of SrO for SiO_2 is beneficial in releasing of ions from the bioactive glasses. This could be attributed to disruption in network connectivity of the glass. It is noteworthy that the pH plays an important role in the deposition of calcium and phosphate (Ca-P) layer and a higher pH leads to the calcium carbonate precipitation [133]. Therefore, an appropriate pH is required for HCA layer formation. Importantly, when the bone forms, the cross linking of the collagen chains and the subsequent precipitation of hydroxyapatite are pH dependent [28,37]. The results of low NCB glasses demonstrate a moderate pH value as compared to Sr-0 and Sr-1, suggesting it highly beneficial during HCA formation and towards various biological processes.

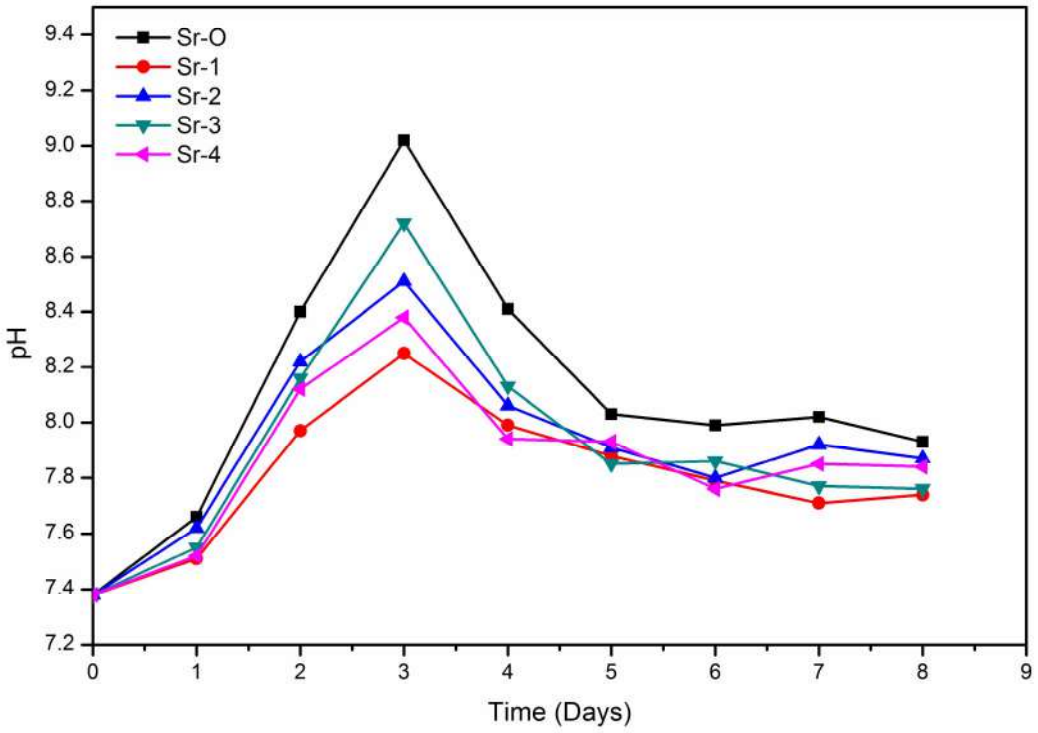

Figure 5.2 pH behaviour of the SBF after immersion of the bioactive glasses (Sr-0, Sr-1, Sr-2, Sr-3 and Sr-4) for different time periods

B. FTIR studies

Figure 5.3 shows the Fourier transform infrared (FTIR) absorption spectra of the bioactive glass samples recorded in the wavenumber range of 400–4000 cm^{-1} on the FTIR spectrophotometer. The parent bioglass® (Sr-0) reveals the FTIR peaks at 445, 863, 986, 1044, 1403 and 1580 cm^{-1}. The spectral bands of Sr-1, Sr-2, Sr-3 and Sr-4 samples have revealed a similar behavior like Sr-0 sample, with small variations in the band intensities. The resultant FTIR band centered at around 445 cm^{-1} is associated with a Si–O–Si symmetric bending mode of vibration in silicate network. The peak at about 863 cm^{-1} is assigned to the $Si\text{-}O^-$ stretching mode of vibration with non-bridging oxygen per SiO_4 tetrahedron (Si-O-2NBO). Another strong shoulder at around 986 cm^{-1} has been attributed to Si–O stretching mode with one non-bridging oxygen (Si-O-1NBO) per SiO_4 tetrahedron [115,134]. It was observed that the intensity of these two peaks centered at 863 cm^{-1} and 986 cm^{-1} has increased in low NCB glasses. The addition of modifiers in the glass breaks the bonds of bridging oxygens (Si-O-Si) of SiO_4 network and produce non-bridging oxygens (NBOs) (Si-O-NBO) [98]. Therefore, these results were found to be in agreement with the substitution of SrO for SiO_2, which creates a high number of non-bridging oxygens. The minor peak observed at 1044 cm^{-1} can be attributed to Si-O-Si asymmetric stretching mode of vibration in the silicate tetrahedral network. The bands at 1403 cm^{-1} and 1580 cm^{-1} are correspond to C-O stretching mode which might have appeared due to reaction between the glass and carbon dioxide present in the atmosphere [115]. However, this phase was not noticed in the XRD.

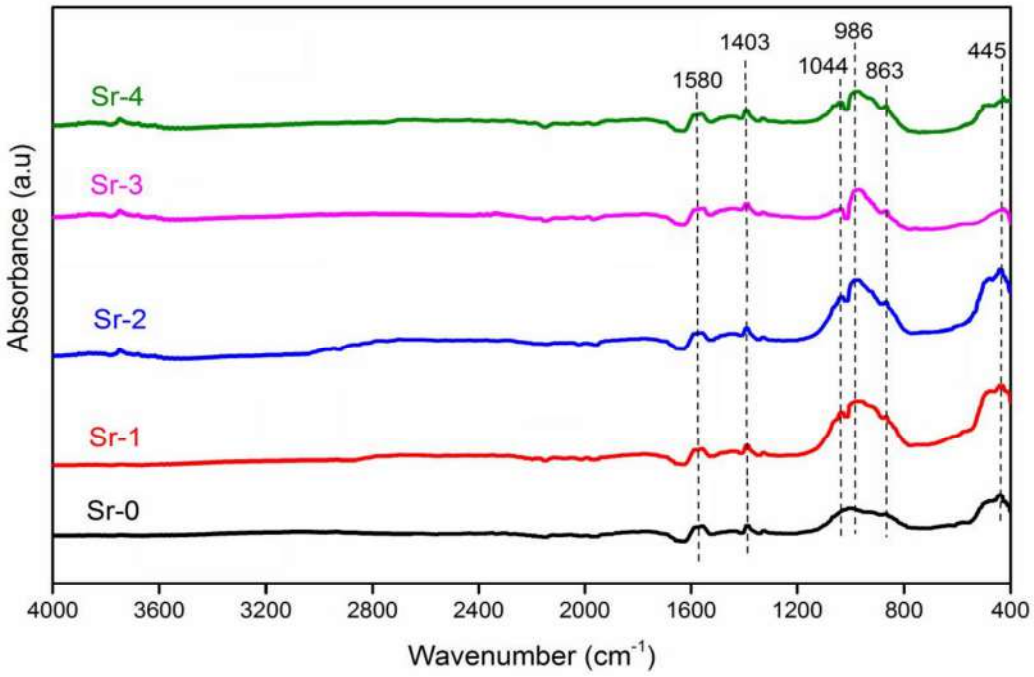

Figure 5.3 FTIR spectra of the bioactive glass samples (Sr-0, Sr-1, Sr-2, Sr-3 and Sr-4) before immersion in SBF.

After immersion of samples in SBF for 7 days, the new bands emerged at 578 cm^{-1}, 1197 cm^{-1}, 1458 cm^{-1} and 3705 cm^{-1} which are shown in **Figure 5.4**. The bands centered at 578 cm^{-1} and 1197 cm^{-1} are attributed to the P-O bending mode of vibrations. Another fresh band appeared at around 1458 cm^{-1} corresponding to C-O stretching mode and it was observed that the intensity of this band has increased in low NCB glasses. A broad band at around 3705 cm^{-1} is assigned to the presence of O-H groups. These characteristic bands represent the formation of hydroxyl carbonate apatite (HCA) layer on the surface of the bioactive glass samples [95,134]. It is noteworthy that the bands at 863 cm^{-1} and 986 cm^{-1} (Si-O-NBO) disappeared after immersion in SBF which is possibly due to the release of cations and simultaneous release of soluble silica from the samples. Therefore, the surface is rich in silica (Si-OH) layer and hence the band intensity increased at 1044 cm^{-1} after SBF treatment

and this peak became more prominent in low NCB glasses. Further, the low NCB glasses are rich in silica-layer which easily accommodates more amounts of carbonates. It is quite evident from the spectra that the intensities of the carbonate groups (1403 cm^{-1} and 1458 cm^{-1}) has increased in these bioactive glasses [135]. Therefore, the results suggest that the HCA layer formation would be more in low NCB glasses.

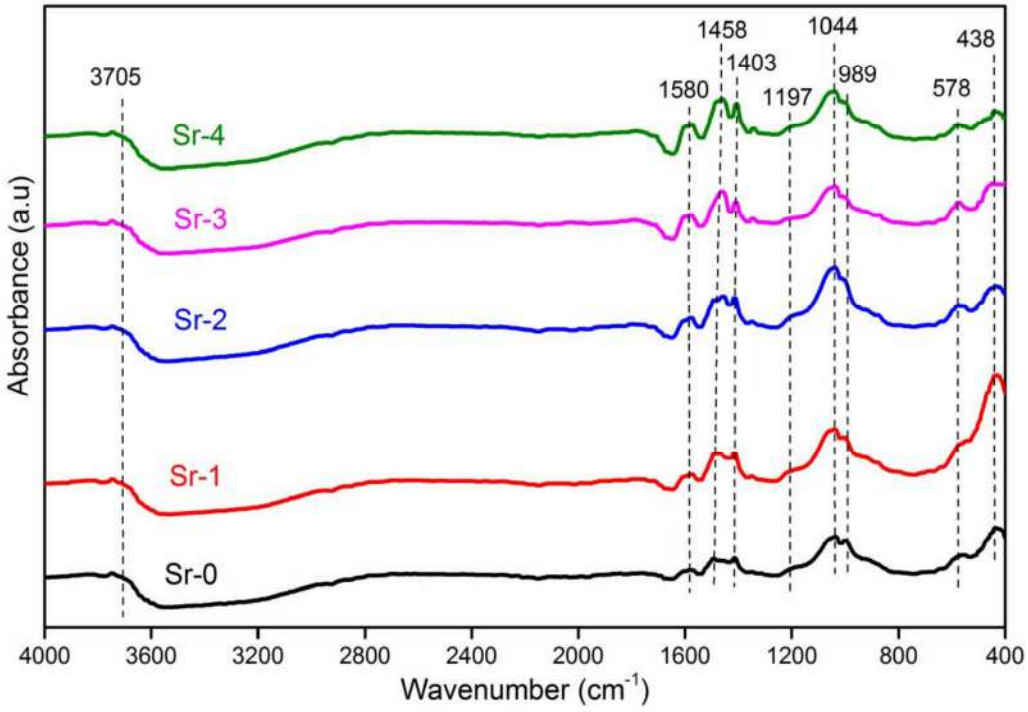

Figure 5.4 FTIR spectra of the bioactive glasses after immersion in SBF for 7 days (Sr-0, Sr-1, Sr-2, Sr-3 and Sr-4).

C. X-Ray diffraction analysis

Figure 5.5 represents the XRD pattern of prepared bioactive glass samples (Sr-0, Sr-1, Sr-2, Sr-3 and Sr-4). The investigation was carried here for the qualitative characterization of bioactive glasses. It is evident from the XRD data that all the bioactive glasses were found to be homogeneous and amorphous in nature. The bulk glasses were optically transparent after melting and casting. Notably, the amorphous

scattering of a broad hump at around 2θ = 32° was found in all the glasses and this hump became more intense as the concentration of SrO increased in Sr-2, Sr-3 and Sr-4 glass samples. This change may be attributed to narrowing the silicate network by larger strontium cations [115].

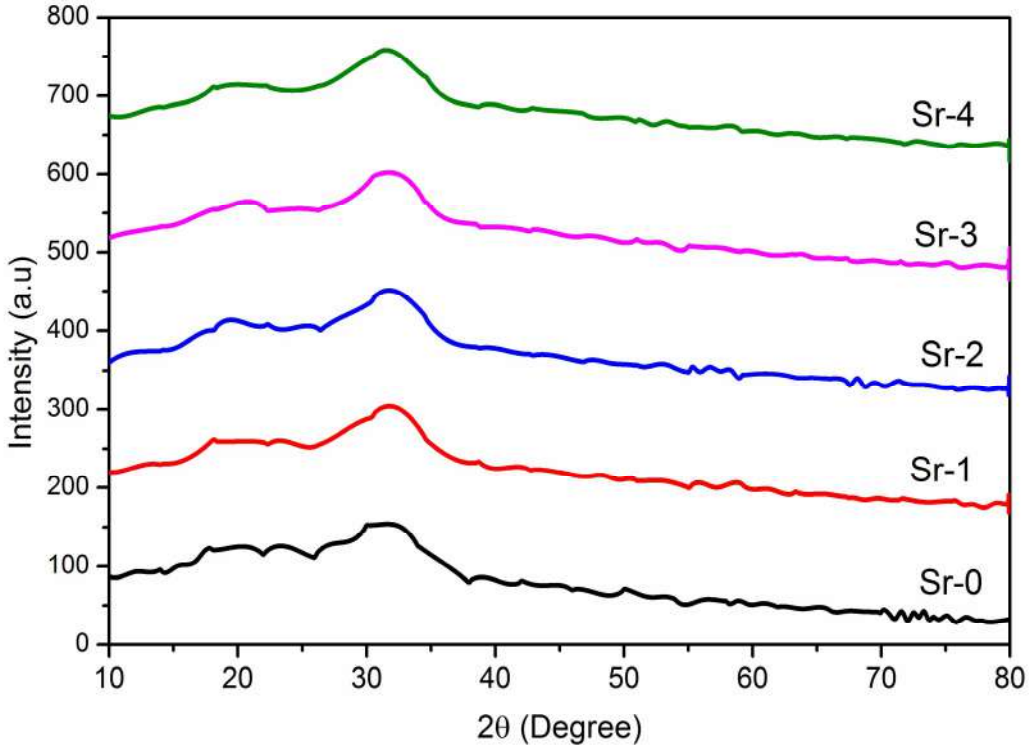

Figure 5.5 XRD pattern of the bioactive glass samples (Sr-0, Sr-1, Sr-2, Sr-3 and Sr-4) before immersion in SBF.

Figure 5.6 shows the XRD patterns of the bioactive glasses after immersion in SBF for 7 days and the results show the formation of crystalline phases after SBF treatment. In general, the bioactivity of the sample is associated with the ability of hydroxy apatite (HA) layer formation on their surface in SBF under physiological conditions. The *hkl* planes (211), (203) and (313) are located at 2θ corresponding to crystalline phase of hydroxyapatite [$Ca_{10}(PO_4)_6(OH)_2$] and the diffraction peaks were matched with the standard PCPDF#: 74-0565 [95,100,131]. Therefore, all the samples

confirm the HA phase formation after immersion in SBF for 7 days. It was observed from the XRD spectra that the intensities of the peak (211) differed with each other and this difference is attributed to the varying amount of phase formed in each sample. It is interesting to discuss here that the parent (45S5) bioglass® sample Sr-0 show calcite as the major phase (2θ = 29.46°, PDF No. 85-1108) as compared to HA phase. Whereas, the Sr-containing glasses did not show the calcite phase, but exhibited the formation of HA. The present trends are well supported by earlier reports that the 45S5 bioactive glass precipitates calcite and hinders the formation of HA layer on the surface [133,136]. Further, it was reported previously that the substitution of SrO for CaO in the bioactive glass retards the HA layer formation in SBF. This is due to the greater M–O bond strength and lower electronegativity (0.99 and 1.04 for Sr^{2+} and Ca^{2+}, respectively) of SrO, which consequently decreases the exchange ability of Sr^{2+} with H^{+} from the solution and this is in conformity with Sr-1 result (**Figure 5.6**) [54,113,130]. This is also is good agreement with pH data which shows a low integral loss (**Figure 5.2**). However, the results demonstrate that the presence of strontium in these bioactive glasses retard the precipitation of calcite layer and favor the formation of HA layer. Further, it is to emphasize that the low NCB glasses display a significant growth of crystalline HA in SBF in comparison to other glasses (Sr-0 and Sr-1). This enhancement may be attributed to the substitution of strontia for silica, which lowers the glass NC. During aqueous attack the leaching of alkali and alkaline earth ions would be much easy and relatively quick in these bioactive glasses, leaving exceedingly silica rich layer (Si-OH groups). This is in good support with the FTIR data displayed a peak at 1044 cm^{-1} after immersion in SBF (**Figure 5.4**). Subsequently, this layer plays an important role in adsorption of calcium and phosphate ions from the solution. Thus, the

more calcium and phosphate (Ca-P) layer could have deposited on surface of these bioactive glasses [29,51,95].

Furthermore, taking the peak (211), the HA crystallite size was calculated using Debye Scherrer formula as given in equation (5.3) [54,55] and was found to be 7.96 nm, 1 5.46 nm, 22.23nm, 38.04 nm and 21.19 nm for Sr-0, Sr-1, Sr-2, Sr-3 and Sr-4, respectively as presented in **Figure 5.6**. Thus, the results confirm the enhancement in HA phase formation in Sr-2, Sr-3 and Sr-4 as compared with other glasses. It is to state that the Sr-4 glass reveals a decrease in the intensity of XRD peak (211) thus resulting in a decrease in crystal size as compared to Sr-2 and Sr-3. It is noteworthy that the sample Sr-4 is expected to show a higher bioactivity because of its lowest NC and highest Sr concentration. But, the result show that high content of the strontium has a destabilizing effect in HCA formation [94]. This could be due to the greater metal-oxygen bond strength and lower electronegativity of strontium, as the concentration of SrO increases in the bioactive glass, the ability of exchange of Sr^{2+} from the solution might have decreased. Moreover, it was depicted by earlier workers that the substitution of SrO for CaO at lower concentration increases the HA crystal size and at higher concentration it decreases [94,130,137]. The similar trend is also observed in these low NCB glasses. Therefore, the results demonstrate that the addition of strontium at lower concentrations favor the HCA formation and higher concentration delays. Hence, the formation of HA is highly dependent on glass structure and therapeutic ions [27,29,58,138,139].

$$D = \frac{0.9\lambda}{\beta\cos\theta} \qquad ----(5.3)$$

Where, D is the grain diameter, λ is the wavelength of the incident X-rays (λ= 0.15406 nm for CuKα radiation), β is the full width at half maximum (FWHM) in radians and θ is the diffraction angle in degrees

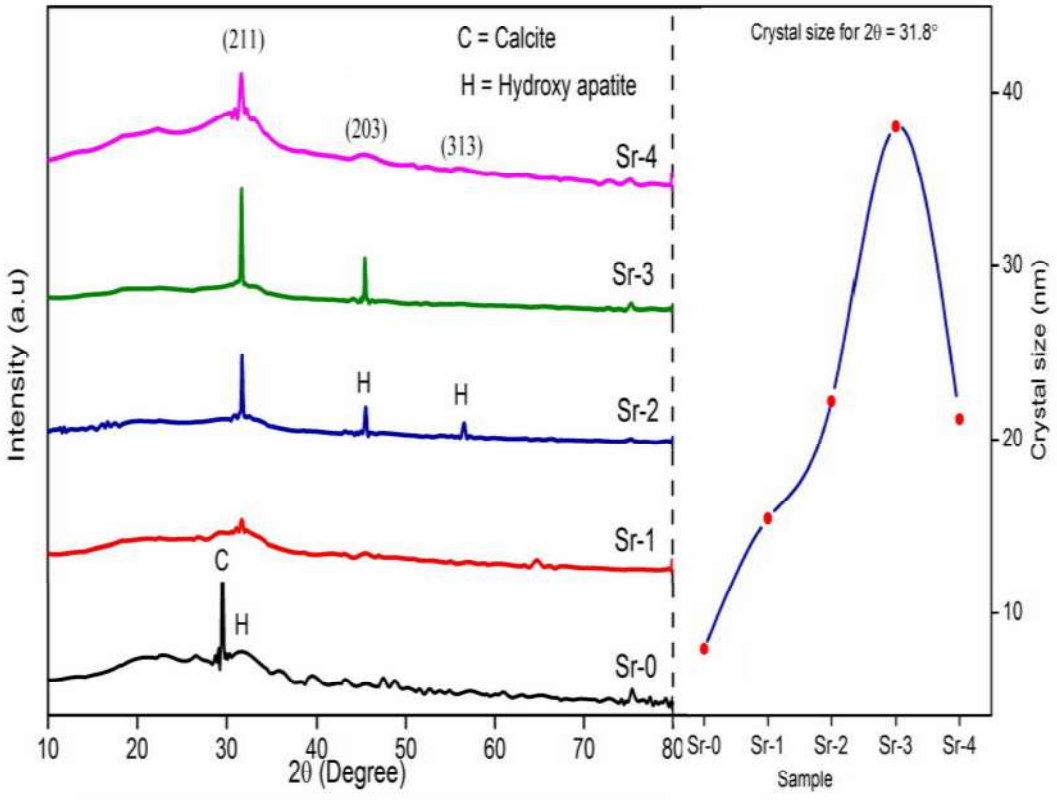

Figure 5.6 XRD pattern of the bioactive glass samples after immersion in SBF for 7 days with HA crystallite size (Sr-0, Sr-1, Sr-2, Sr-3 and Sr-4)

D. Surface morphology of the bioactive glasses by SEM and EDS

Figure 5.7 (A-E) shows the SEM images of Sr-0, Sr-1, Sr-2, Sr-3 and Sr-4 samples and all of them represent the glassy nature before immersion in SBF. **Figure 5.7 (F)** shows the EDS spectra of Sr-3 which indicated the elements Si, Ca, Na, P and Sr being present on the surface of the sample and their concentrations have been presented in **Table-5.2**. **Figure 5.8 (A-E)** shows the SEM micrographs of the bioactive glasses

(Sr-0, Sr-1, Sr-2, Sr-3 and Sr-4, respectively) after the immersion in SBF for 7 days. A change in surface morphology is seen if compared with the initial surface of the samples. The SEM micrographs demonstrate that spherical particles have covered the surface of the bioactive glasses with variable shape and size. The EDS analysis was done on the surface of Sr-3 after immersion in SBF for 7 days (**Figure 5.8 F**). The result shows that the spherical particles contained C, Ca, P and Sr with high intensity and Si with low intensity peaks when compared with the initial surface (**Figure 5.7 F**). This significant increase in C, Ca, and P as well as a decrease in Si intensities indicate the formation of hydroxy carbonate apatite (HCA) layer [26]. This is also in good conformity with the EDS elemental concentrations which show a decrease in Na and Si as well as an increase in Ca, P and Sr as shown in **Table 5.2**. Therefore, the EDS spectra further have confirmed the growth of HCA crystals on the surface of the samples after immersing in SBF. It is interesting to note that the Sr^{2+} ion was detected in the newly formed spherical particles which suggests that the strontium ion is partially substituted for calcium in HCA to form Sr-HCA [94,140]. It was also observed that the numbers of HCA crystals are more on the surface of Sr-2, Sr-3 and Sr-4 as compared with other bioactive glasses. This significant development of HCA crystals might be associated with a high deposition of Ca-P layer which is in good conformity to the XRD analysis (**Figure 5.6**). It is noteworthy that the surface energy of a material is defined by its general charge density and the net polarity of the charge of the elements present [141]. The substitution of SrO for SiO_2 not only reduces the NC but also decreases the surface charge of the glasses. It is also an important variable to considered that the surface energy of the biomaterial influences on protein and cells adherence [118]. Hence, a significant growth in HCA crystals is evident from SEM micrographs of Sr-2, Sr-3 and Sr-4 samples.

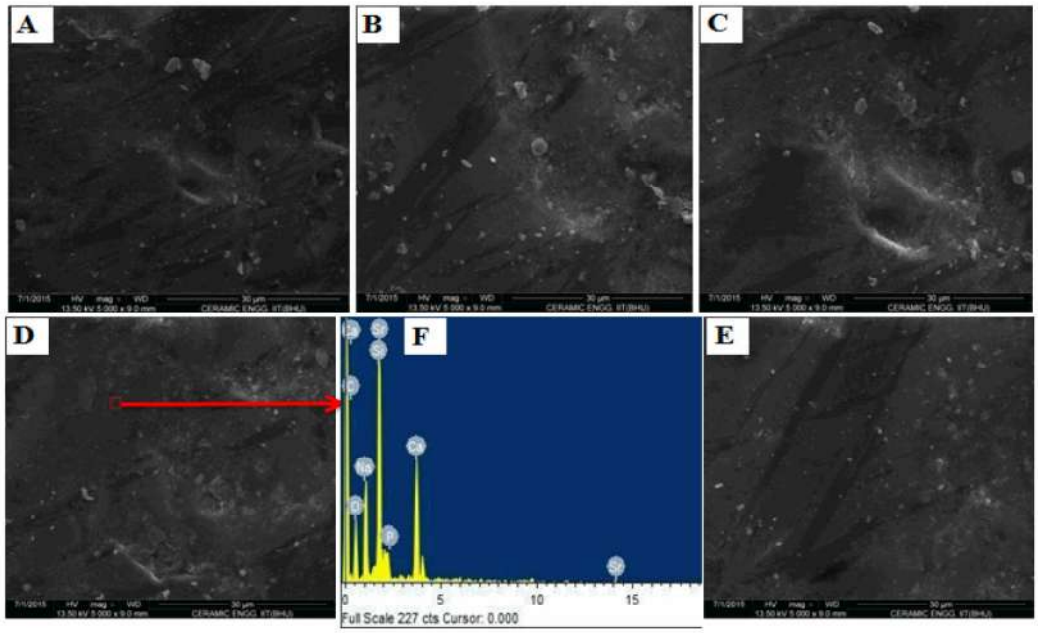

Figure 5.7 SEM micrographs of the bioactive glasses before immersion in SBF (A) Sr-0, (B) Sr-1, (C) Sr-2, (D) Sr-3, (E) Sr-4 and (F) EDS spectra of Sr-3.

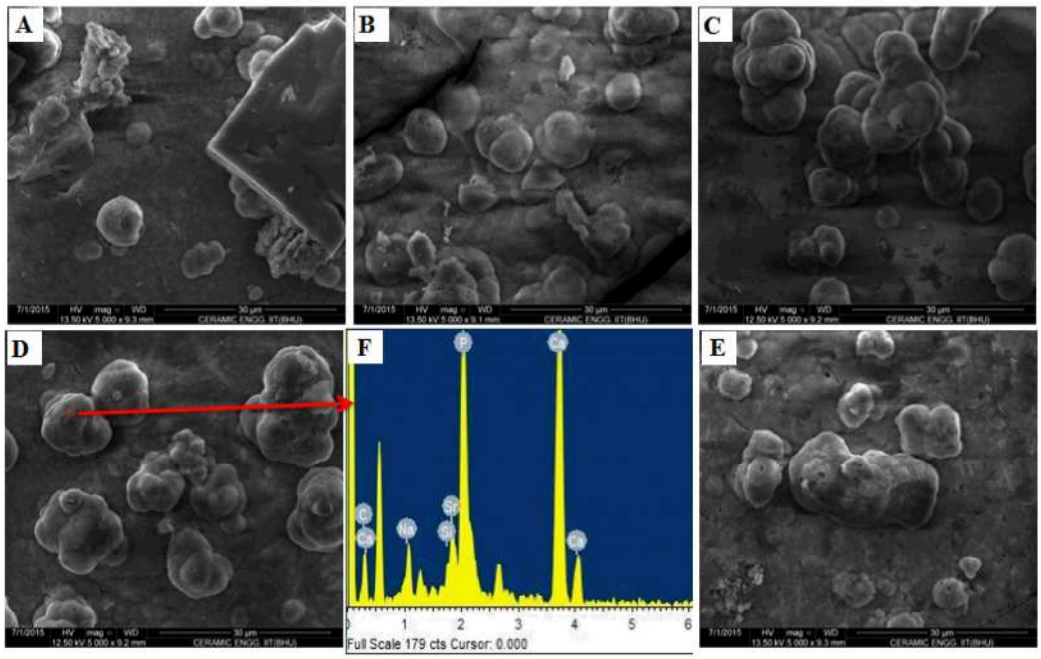

Figure 5.8 SEM micrographs of the bioactive glass surfaces after immersion in SBF for 7 days (A) Sr-0, (B) Sr-1, (C) Sr-2, (D) Sr-3, (E) Sr-4 and (F) EDS spectra of Sr-3.

Table 5.2 Elemental analysis of Sr-3 sample before and after SBF treatment by EDS.

Before SBF treatment				After SBF treatment		
Elements	**Weight (%)**	**Atomic (%)**		**Elements**	**Weight (%)**	**Atomic (%)**
Na K	15.15	21.44		Na K	9.00	14.32
Si K	38.58	44.71		Si K	1.02	1.33
P K	7.47	7.85		P K	32.81	38.71
Ca K	26.29	21.35		Ca K	44.06	40.17
Sr L	12.52	4.65		Sr L	13.11	5.47
Total	100.00	100.00			100.00	100.00

5.3.3 Mechanical properties

A. Compressive and flexural strength of bioactive glasses

It is important to note here that the mechanical stability is required for implant biomaterials, essentially for large bone defects to resist the mechanical stress caused during the clinical surgery and from implantation to complete conversion of HA [111]. We have reported the mechanical properties in two different methods namely destructive (compressive) and non-destructive (Young's modulus, bulk modulus and shear modulus) for better understanding and conclusions of the samples. In order to investigate the mechanical behavior, the bulk glass samples were cut into required dimensions, ground and polished to get an optically transparent surface as shown in **Figure 5.9** inset which is described in the text. The compressive and flexural strengths of the bioactive glasses (Sr-0, Sr-1, Sr-2, Sr-3 and Sr-4) have been presented in **Figure 5.9**. It is found that both compressive and flexural strengths of Sr-1 increased as compared to Sr-0 besides the same quantity of the modifiers in both the glasses (Sr-0 and Sr-1). This could be due to the partial substitution of bigger Sr^{2+} ion at the cost of a

smaller Ca^{2+} ion in glass network (ionic radius of Sr^{2+} and Ca^{2+} are 2.15Å and 1.97Å, respectively). This means the presence of larger Sr^{2+} ion in the system increases the interference in the glass network. Thus, it leads to an increase in compactness of the glass structure which might have resulted in better strength. Further, it is observed that both the strengths increased significantly with increasing the concentration of SrO for SiO_2 (Sr-2, Sr-3 and Sr-4). Similarly, the substitution of larger Sr^{2+} (2.15Å) ion for a smaller Si^{4+} (1.11Å) ion in glass network increases the packing density. Mostly, the modifiers like Mg^{2+}, Ca^{2+}, Sr^{2+} and etc. occupy the interstitial positions in the glass structure [112]. This is in good conformity with the density results, which showed an appreciable increase with increasing the concentration of SrO as shown in **Table 5.3**. This confirms the close packing of atoms increases the compactness of the glass structure which might have resulted in significant improvement in both compressive and flexural strengths. Moreover, it was also observed from earlier studies [86,95,99,112] that glasses containing high amount of modifiers have shown better mechanical properties.

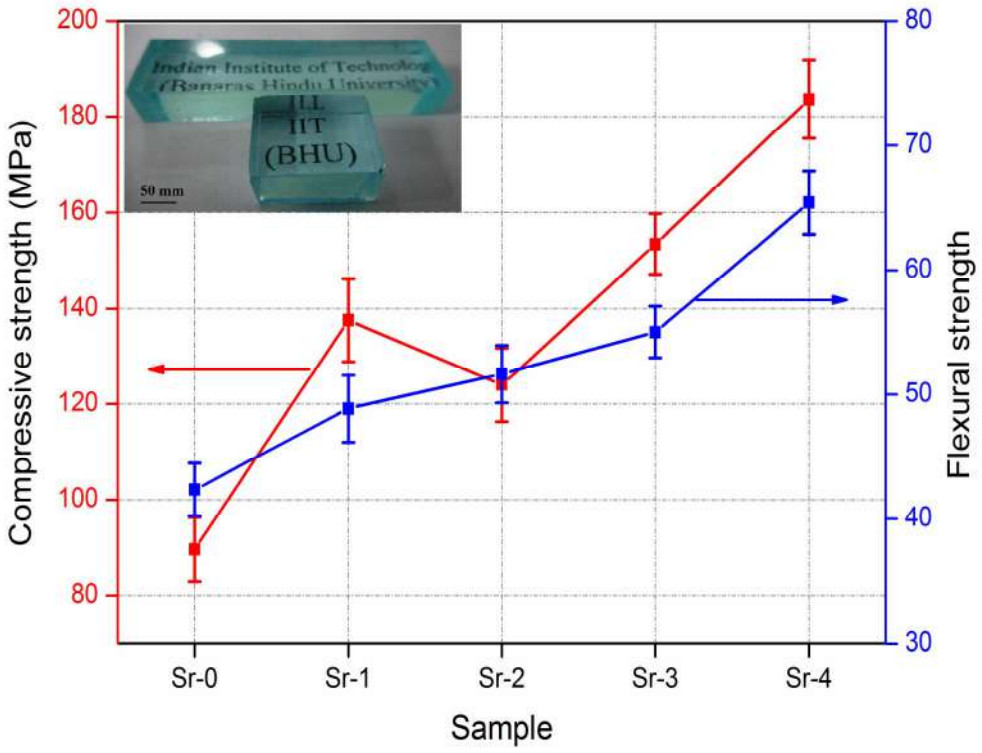

Figure 5.9 Compressive and flexural strengths of the bioactive glass samples (Sr-0, Sr-1, Sr-2, Sr-3 and Sr-4)

B. Modulus of elasticity

We have also reported the mechanical behavior of the samples in non-destructive model namely, Young's modulus (E), shear modulus (S) and bulk modulus (K). In order to investigate the mechanical behavior, the bulk glass samples were cut, ground and polished to get an optically transparent surface as shown in **Figure 5.10** inset [written text]. Young's, bulk and shear modulus (Elastic moduli) of the bioactive glasses (Sr-0, Sr-1, Sr-2, Sr-3 and Sr-4) have been presented in **Figure 5.10**. The elastic moduli of Sr-1 sample have increased as compared to Sr-0 sample besides the equal quantity of modifiers in both the glasses (Sr-0 and Sr-1). The possible reason could be associated with the partial substitution of bigger Sr^{2+} ion at the cost of a smaller Ca^{2+} ion in glass network (ionic radius of Sr^{2+} and Ca^{2+} are 2.15Å and

1.97Å, respectively); That means the presence of larger Sr^{2+} ion in the system increases the interference of the glass network. Therefore, the reduction in interatomic spacing results in the densification of Sr-1. Thus, it leads to an increase in compactness of the glass structure which might have resulted in an increase in elastic moduli.

Further, the Sr-2, Sr-3 and Sr-4 bioactive glass samples have shown significant increase in elastic moduli in comparison to Sr-0 and Sr-1. The reason for this superior strength could be associated with the substitution with larger Sr^{2+} (2.15Å) ion for a smaller Si^{4+} (1.11Å) ion in glass network. Hence, the packing density increased significantly in these bioactive glasses. This is in good conformity with the density results of the samples. The density of the bioactive glasses increased appreciably while a linear decrease in oxygen density with increasing concentration of SrO was also observed and it can be seen in **Figure 5.11**. The oxygen density of the bioactive glass was calculated with the following equation (2) in order to measure the compactness of the glass structure according to earlier reports [48,115]. This confirms the close packing of atoms in the bioactive glasses. Mostly, the modifiers like Mg^{2+}, Ca^{2+}, Sr^{2+} and etc. occupy the interstitial positions in the glass structure and as the concentration of SrO increases the compactness of the glass structure also increases [112]. Therefore, the average number of the network bonds per unit volume increases in the glass structure [99,112,114]. Hence, the propagation of sound wave in a compacted glass could be much faster which resulted in the improvement in elastic moduli. Moreover, it was also observed from earlier studies [42][54]–[57] that the glasses containing higher amount of modifiers have shown better mechanical properties.

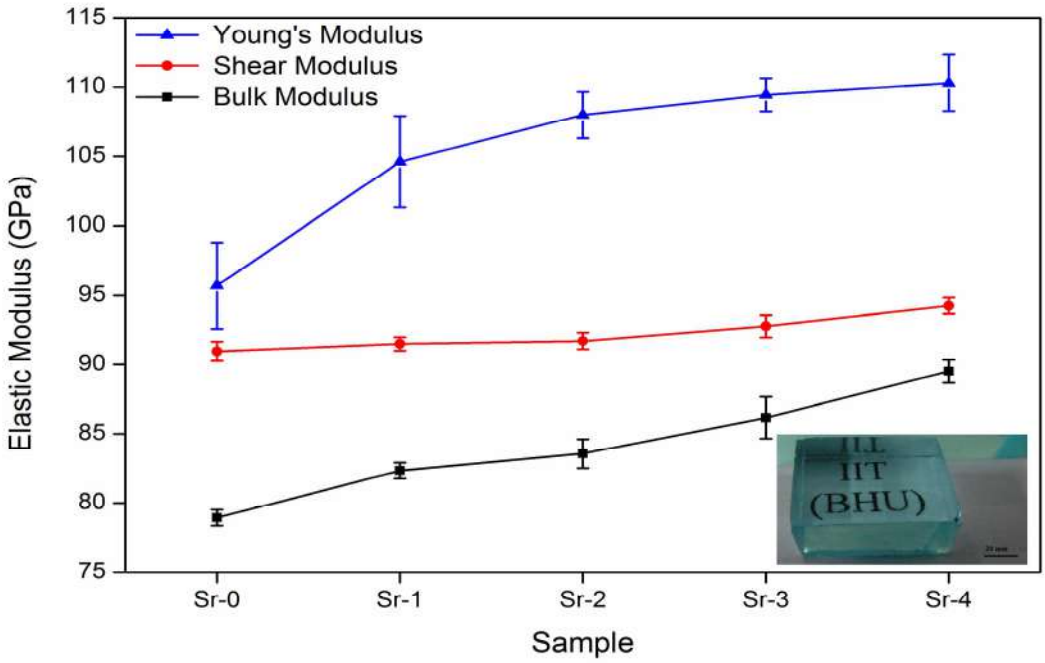

Figure 5.10 Young's Modulus, shear modulus and bulk modulus of the bioactive glass samples (Sr-0, Sr-1, Sr-2, Sr-3 and Sr-4.

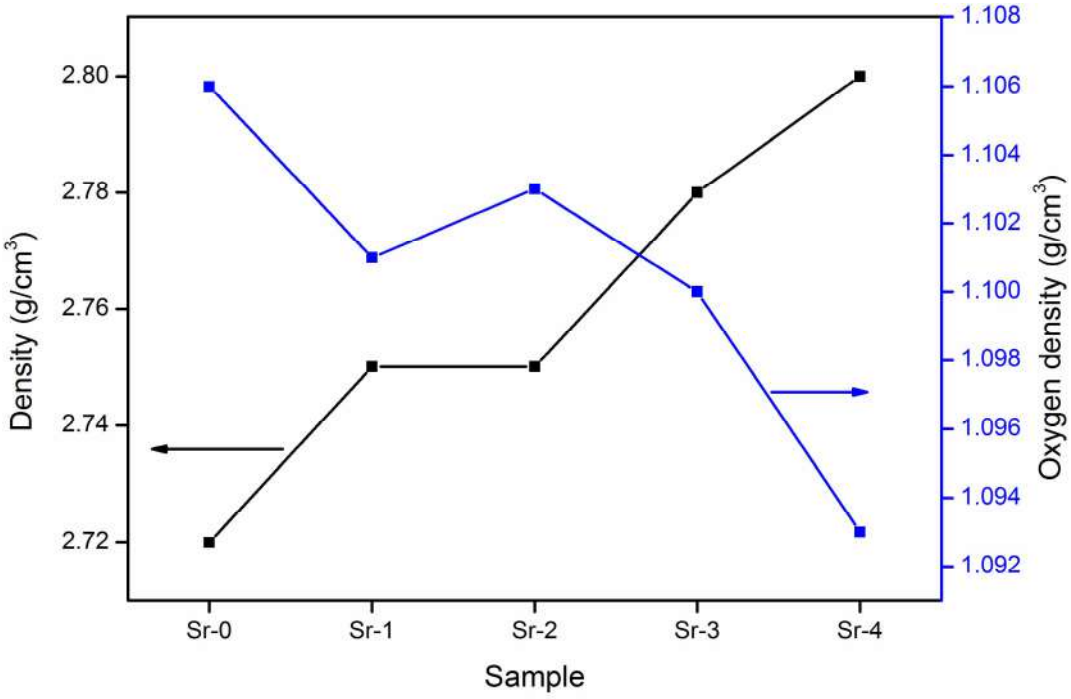

Figure 5.11 The variation in density and oxygen density of the bioactive glasses (Sr-0, Sr-1, Sr-2, Sr-3 and Sr-4)

Table 5.3 Glass density, oxygen density and elastic modulus (Young's, Bulk and Shear modulus) of bioactive glass samples (Sr-0, Sr-1, Sr-2, Sr-3 and Sr-4).

Samples	Glass density (g/cm^3)	Oxygen density (g/cm^3)	Young's Modulus (GPa)	Shear modulus (GPa)	Bulk Modulus (GPa)
Sr-0	2.72	1.106	78.93 ± 0.59	31.97 ± 0.71	50.26 ± 5.11
Sr-1	2.75	1.101	82.34 ± 0.27	32.51 ± 0.50	59.16 ± 5.38
Sr-2	2.75	1.103	83.56 ± 1.04	32.72 ± 0.61	62.52 ± 1.67
Sr-3	2.78	1.100	86.16 ± 1.51	33.78 ± 0.80	63.99 ± 1.20
Sr-4	2.80	1.093	89.51 ± 0.85	35.25 ± 0.58	64.85 ± 2.04

5.3.4 Assessment of biocompatibility

A. Cell Viability

On the basis of bioactivity in SBF and mechanical properties of Sr-contained and Sr-free bioactive glasses, the Sr-substituted glasses have shown better bioactivity and better mechanical strength as compared to Sr-0. Therefore, only the Sr substituted glasses were taken for biological study. The *in vitro* cell culture studies were carried out using human osteosarcoma U2OS cell lines and assessed the cell viability, proliferation and blood compatibility. In general, most of the biomaterials at lower concentrations can exhibit biocompatibility during *in vitro* cell culture studies. The higher concentration of the sample can furnish better information and conclusions for the compositional effect. Cell viability of the Sr-containing samples (Sr-1, Sr-2, Sr-3 and Sr-4) was assessed against U2OS cell lines by XTT viability assay. **Figure 5.12** shows the percentage cell viability with different concentrations of the samples incubated for 24 h at 37°C in 5% CO_2. The percent viability was calculated by considering the

viability of tumor cell cultured in complete medium only as 100%. The cell viability after 24 h exposure to the sample (5mg/ml) was recorded as (85.18 ± 1.79), (95.60 ± 1.35), (96.86 ± 2.11) and (92.24 ± 2.07)% for Sr-1, Sr-2, Sr-3 and Sr-4, respectively. The results have shown that all the samples are cytocompatible at lower concentrations. This is in good agreement to the earlier reports that the strontium substituted bioactive glasses do not affect the cell compatibility [52–55,88]. However, we have also carried out similar studies at higher concentrations (10, 25, 50, 100, 250 and 500 mg/ml) of the samples cultured for 24 h**.** The quantitative results exhibited that the cell viability has decreased with all the samples as their concentration (mg/ml) increased. But, the sample Sr-1 exhibits the drastic fall in cell viability as compared to other samples at a concentration of 500 mg/ml. The Sr-1 was found to exhibit cytotoxicity at higher concentrations on the U2OS cell lines. Whereas, the low NCB glasses demonstrate more than 75% cell survival. This enhancement might be associated with the controlled release of ions from the glass surface, which played an important role in cell lines survival [53,92]. The low NCB glasses could have released an appropriate amount of ions and created a better environment for survival of the cells. These results suggest that the substitution of SrO for SiO_2 has improved the cell compatibility more than SrO for CaO. This effect could be seen with Sr-1 at any of the concentrations studied presently. Moreover, the sample Sr-3 possessed significant cell viability (86%) even at higher concentration (500 mg/ml). The Sr-3 sample contains 2.0 mol% of strontium with NC as 1.94 suggesting that might be the optimal concentration in these series of glasses.

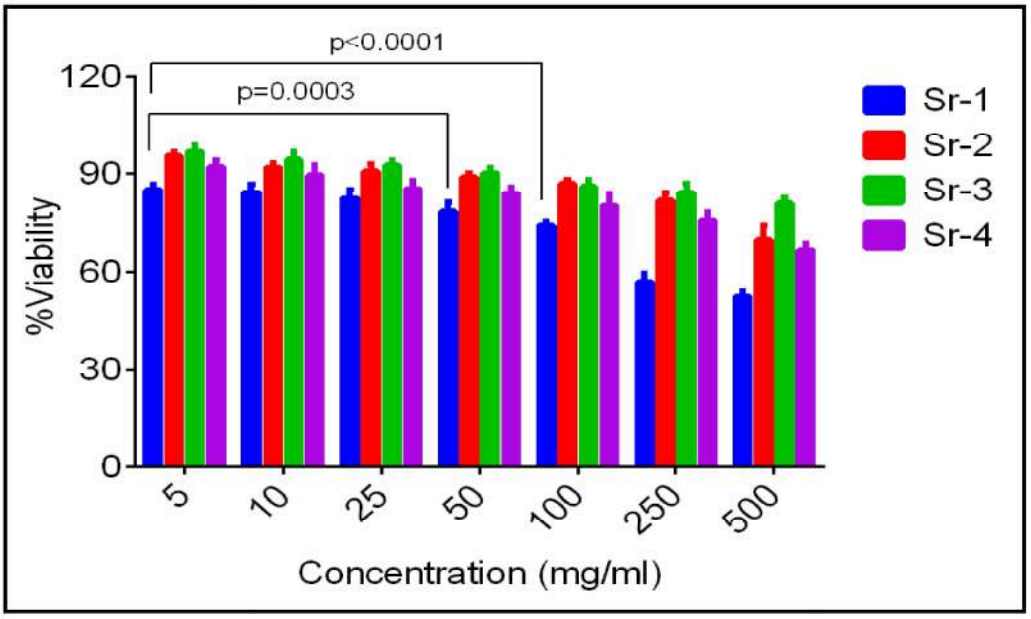

Figure 5.12 (A) Viability of Sr-contained bioactive glasses against U2-OS cells was studied following MTT viability assay (Promega, USA). 5×10^3 cells were plated in 96 well plates and were cultured in complete medium in presence of Sr-contained bioactive glasses with different concentrations for 24 h.

B. Cell cytotoxicity

The non-radioactive cytotoxicity assay was used to assess the toxicity of strontium containing samples on U2OS cell lines and the percentage cytotoxicity was reported in **Figure 5.13.** The cell cytotoxicity after 18 h exposure to sample (5mg/ml) was recorded as (15.72 $\pm$ 3.41), (8.07 $\pm$ 2.90), (4.35 $\pm$ 1.49) and (12.94 $\pm$ 3.59)% for Sr-1, Sr-2, Sr-3 and Sr-4, respectively. The results show that all the samples have been found to be cytocompatible at lower concentrations. This is in good conformity with the earlier reports that the strontium substituted bioactive glasses did not show cell toxicity [52–55,88]. In general, according to *in vitro* cell culture studies most of the biomaterials at lower concentrations can exhibit cytocompatibility. However, the higher concentration of the sample can furnish better information and conclusions for

the compositional effect. Similar study was carried out with higher concentrations (10, 25, 50, 100, 250 and 500 mg/ml) of the samples cultured for 18 h. The results exhibit that the cell cytotoxicity was found to increase with increasing the concentration (mg/ml) of the sample. However, the reference glass sample (Sr-1) shows high cytotoxicity at all the concentrations in comparison to low NCB glasses (Sr-2, Sr-3 and Sr-4). This enhancement in cell compatibility might be associated with the controlled release of ions from the glass surface, which play an important role in cell lines survival [53,92]. This agrees well with the present pH values (**Figure 5.2**) that these glasses show moderate ions dissolution in comparison to Sr-0 and Sr-1 samples. The substitution of SrO for CaO controls the ion release [113,130], whereas substitution for SiO_2 exhibits controlled biodegradability. Furthermore, it is interesting to note that the Sr-1 and Sr-3 samples contain (2.0 mol%) same amount of strontium. But, Sr-3 demonstrates a significant cytocompatibility and this can be seen at all the concentrations tested such as at 500 mg/ml (51.32 ± 1.38) and (18.16 ± 2.85) for Sr-1 and Sr-3, respectively. Therefore, the results suggest that the substitution of SrO for SiO_2 has improved the cell compatibility significantly.

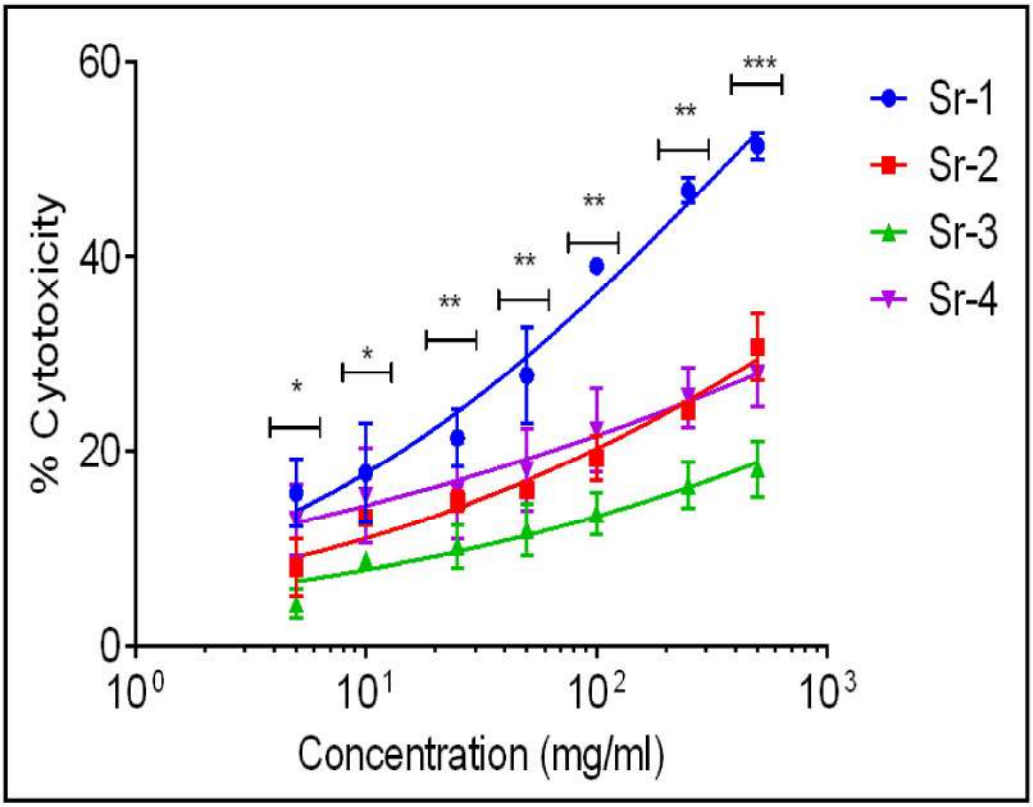

Figure 5.13 Cytotoxicity of Sr-1, Sr-2, Sr-3 and Sr-4 bioactive glasses against osteosarcoma U2-OS cells determined by 18h LDH release assay. Data presented as mean ± SD of triplicate determination.

C. Cell Proliferation

The cell proliferation assay was carried out using U2OS cell lines in two different models; such as various concentrations (5, 10, 20, 50 and 100 mg/ml) of the glasses for 48 h and prolonged periods of time (24, 48, 72 and 120 h) as shown in **Figures 5.14 (A & B)**, respectively. It was observed that the cell growth increased in the presence of all the samples after 48 h of incubation at different concentrations (5, 10, 25, 50, 100, 250 and 500 mg/ml). Moreover, it was noticed that cell proliferation significantly increased in presence of Sr-2, Sr-3 and Sr-4 samples as compared to Sr-1 in both the cases; concentration and time dependant models as presented in **Figures 5.14 A & B,** respectively. It is was reported that the NC of the bioactive glasses pay an

important role in HCA growth [25,29,142]. This is in agreement with low NCB glasses, which demonstrate better cell growth. The controlled rate of release of ions from the sample into biological fluid plays a vital role in cell survival and growth [55,92,132]. Probably, the rate of release of ions from the low NCB glasses might be appropriate. Therefore, the substitution of SrO for SiO2 may be greatly beneficial. Furthermore, it is to emphasize that sample Sr-3 possessed a significant cell growth ($77.29 \pm 3.57\%$) even at higher concentration (500 mg/ml) and longer duration in comparison with the rest of the samples. It is interesting to discuss herewith that the cell growth was favored in low NCB glasses; but decreasing the NC (1.84 for Sr-4) seems to hold up the proliferation and this behavioral trend could be seen in both the models. It was reported earlier that the NC below 1.80 decreases the bioactivity [25,138]. The similar effect was also observed in present investigation for Sr-4 as the NC approaches 1.8. Thus, the results suggest that the NC influences the cell survival and growth and signify a potential scope in bone regeneration.

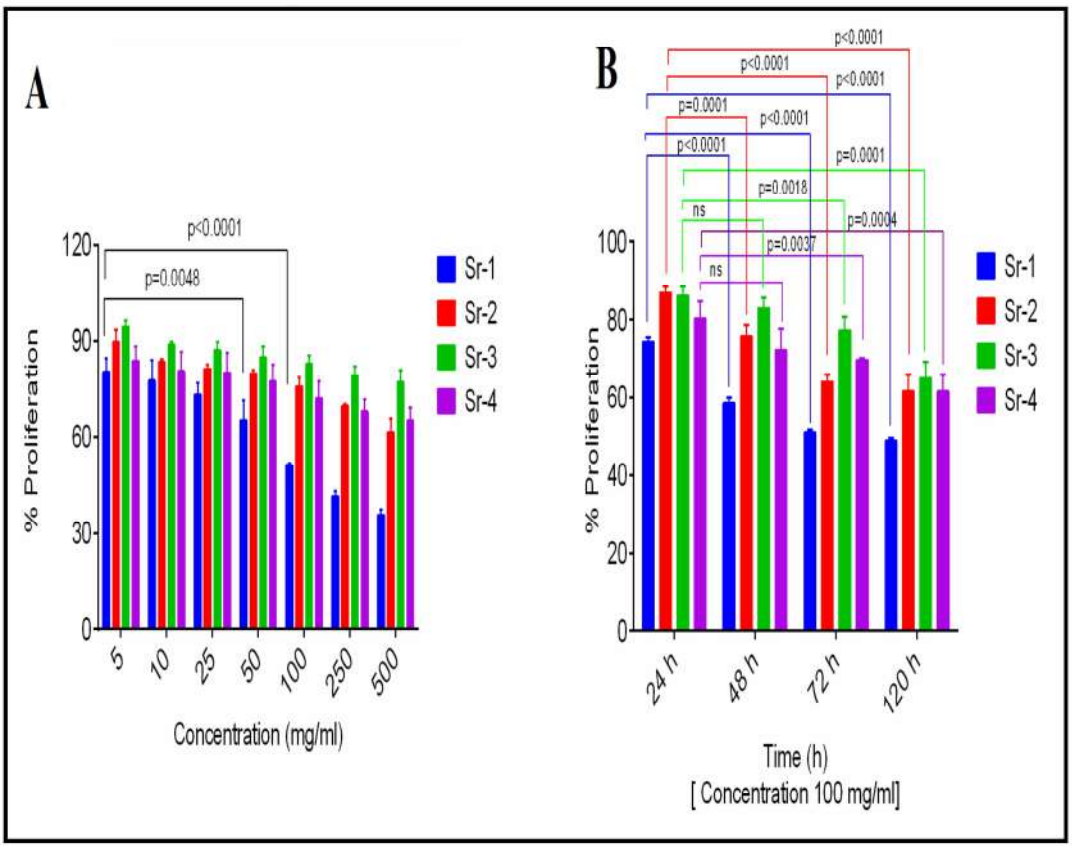

Figure 5.14 (A) Sr-contained bioactive glasses response on cell proliferation and growth of U2-OS cells following co-culture for 48h with different concentrations of the samples. (B) Co-culture with samples for longer duration at constant concentration (100 mg/ml). Data presented as mean ± SD, n = 4.

D. Detection of cell apoptosis

Qualitative assessment of cell apoptosis has been carried out also in presence of the Sr-contained bioactive glasses. The broad spectrum growth inhibition by samples has raised the question whether it can also cause apoptosis of the tumor cells. The fluorescence images of cell morphology of all the Sr-contained glasses have been shown in **Figure 5.15**. It may be reasonable to consider that the inhibitory activity of the samples sometimes may cause cytotoxic effect. Therefore, apoptosis was determined by monitoring changes in the cell size and externalization of

phosphatidylserine of the U2OS cells. The fluorescence images show the cell apoptosis with Sr-1 and Sr-4 samples as compared to Sr-2 and Sr-3 samples.

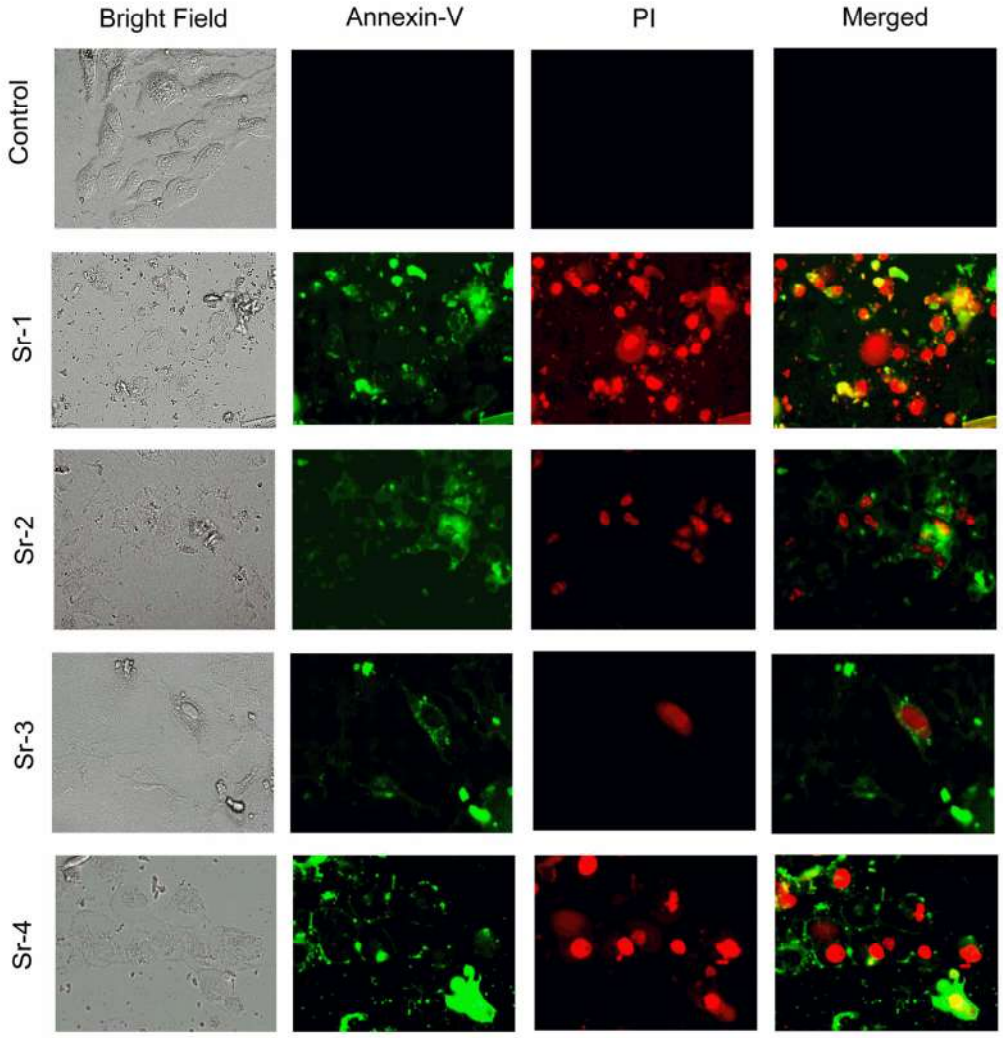

Figure 5.15 Microscopic analysis of induction of apoptosis. U2-OS cells were given indicated treatment with Sr-contained bioactive glasses at a concentration of 5.0 μM, in complete RPMI 1640 medium for 8h at 37°C. The FITC-conjugated Annexin V and Propidium iodide (PI) stained apoptotic cells were visualized under a fluorescence microscope (Nikon Eclipse 80i, Nikon, Japan) with Plan Fluor, 40X, NA 0.75 objective equipped with green and red filters for FITC and PI, respectively. n=4

E. Cell attachment

Figure 5.16 (A-B) shows the SEM and **(C-D)** EDS of the Sr-1 and Sr-3 bioactive glass surfaces after culture for 5 days. There was an excellent attachment and spreading of cells on the surfaces of the bioactive glasses. The change in surface morphology is seen if it is compared with the initial surfaces of the samples. Similarly, the EDS analysis was done after culture for 5 days on the Sr-1 and Sr-3 samples. The EDS results show that the newly formed crystals contain C, Ca, P and Sr with high intensity and Si with low intensity peaks when compared with the initial spectra (**Figure 5.7 F**). This significant increase in C, Ca, and P as well as a decrease in Si intensities indicate the formation of hydroxy carbonate apatite crystals. It is noteworthy that the substitution of SrO for SiO_2 not only decreases the network connectivity but also decreases the surface energy. The surface energy of a material is generally defined by its charge density and the net polarity of the elements present (field strengths of Sr^{2+} and Si^{4+} are 0.30 and 1.57, respectively) [141]. It was mentioned earlier that the decrease in surface tension increases the hydrophilic nature of the sample and hence increases the cell recruitment [40]. Further, the newly developed crystals show the presence of strontium and it indicates that the strontium ion might be partly substituted in Ca-P layer to form $(Ca,Sr)_{10}(PO_4)_6(OH)_2$ [94,140]. It was reported previously that the Sr-contained HA layer exhibited a superior biological response *in vitro* and *in vivo* [93] and thus these samples are in conformance with cell cytotoxicity, proliferation and attachment.

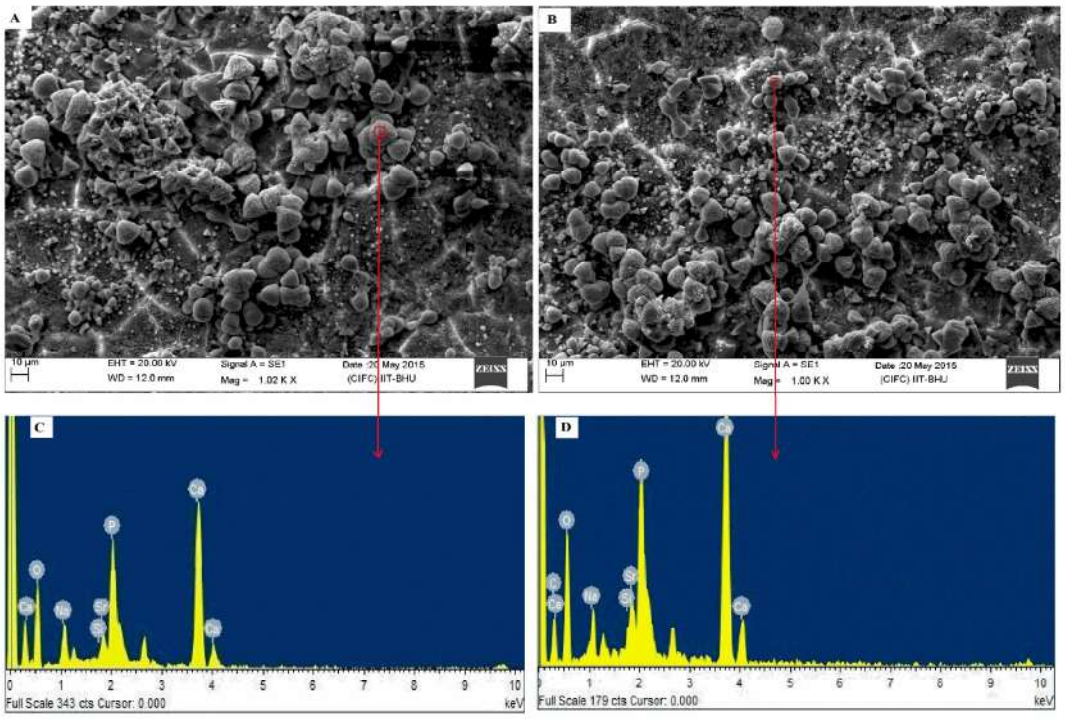

Figure 5.16 SEM images showing osteosarcoma U2OS cells attachment and growth on (A) Sr-1 and (B) Sr-3 bioactive glasses after 5 days culture and their respective EDS spectra of (C) Sr-1 and (D) Sr-3 bioactive glasses (region marked on the images taken for EDS).

F. Hemolysis assay, RBC integrity and size distribution

Hemolysis takes place when the red blood cells (RBC) come in contact with materials and it is important to check the biomaterials before their clinic trials. Hence, the *in vitro* blood compatibility of the Sr-contained bioactive glasses was determined by % hemolysis. The hemolysis experiment has been conducted for prolonged time periods (0.5, 1, 2 and 4 h) and at different concentrations (10, 25, 50, 100, 200 and 500 mg/ml) of the samples. The % hemolysis caused by the Sr-contained bioactive glass samples was presented in **Figures 5.17 A and B** for longer duration of time and concentration depended models, respectively. These results furnish the clear

understanding of the effectiveness of glass compositions on blood compatibility. The results confirm that the strontium contained (Sr-1, Sr-2, Sr-3 and Sr-4) samples did not affect RBC with respect to hemolysis at increasing time point. These results are well within the limits (less than 5%) [143], even after 4 h in contact with blood (**Figure 5.17A**). It was found that the % hemolysis has increased considerably with increasing time and concentrations with Sr-1 sample, while the low NCB glasses exhibited still lower hemolysis in both models (**Figure 5.17 A & B**). It is noteworthy to discuss here that, in the case of low NCB glasses, the Sr-4 exhibited no hemolysis after 30 min of exposure but after 1 h highest % hemolysis was reported amongst low NCB glasses and further it was lowest after at 2 h. This confirms that the ions released from the bioactive glasses at a controlled rate and causing hemolysis. It is to emphasize that, at higher concentrations (250 and 500 mg/ml), Sr-1 causes partial hemolysis (more than 5%), whereas the Sr-2, Sr-3 and Sr-4 glass samples revealed superior blood compatibility which did not even exceed the value by more than 2% (**Figure 5.17 B**). Thus, the low NCB glasses are significantly tolerant to the RBC and could be considered as non-hemolytic. The microscopic observations also demonstrate no change in morphology in RBC following contact with the strontium contained glasses except Sr-1 which show some degree of hemolysis of RBC (**Figure 5.17 C**). Therefore, the results imply that the substitution of strontium at the cost of silica demonstrated better blood compatibility.

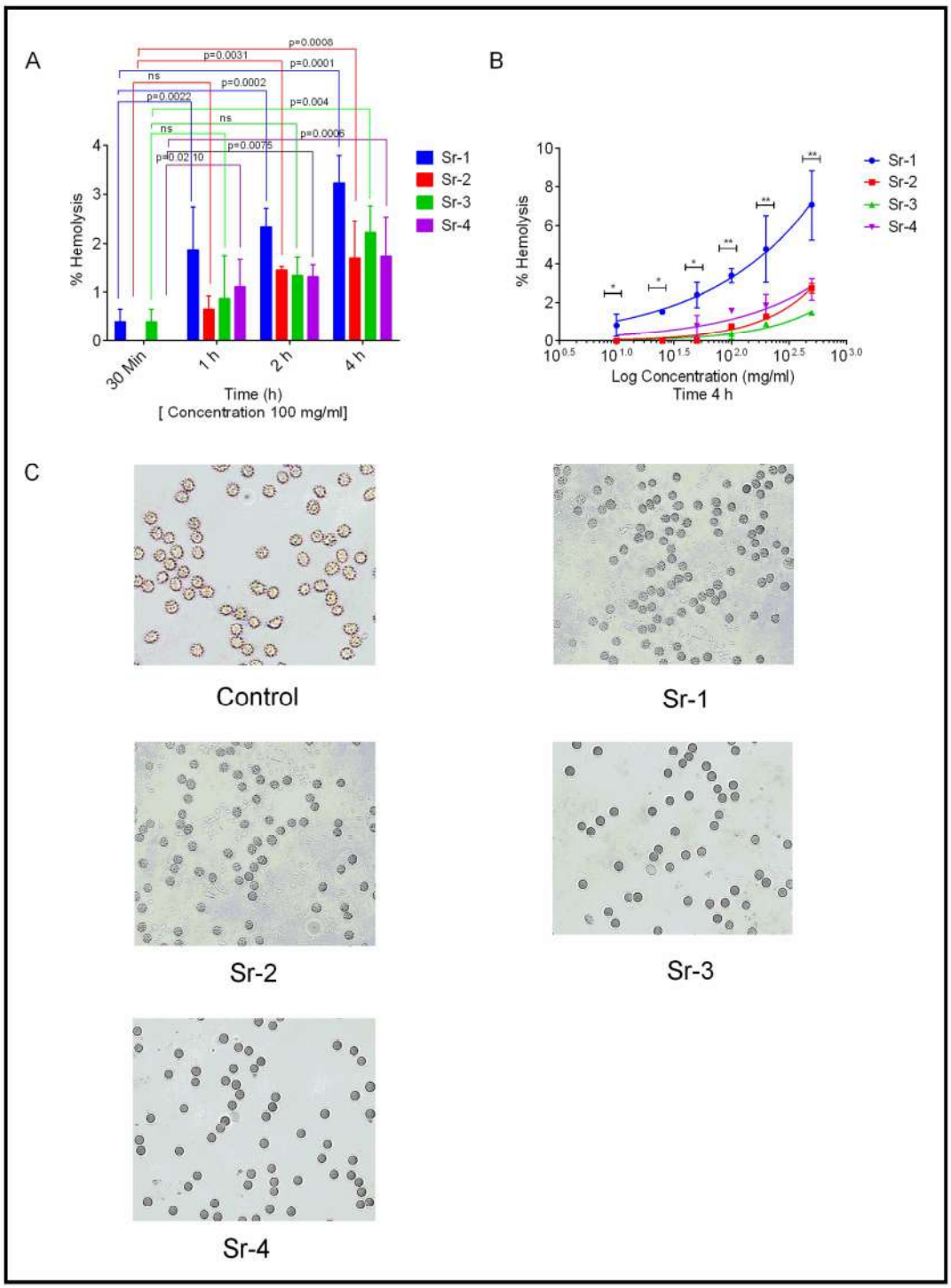

Figure 5.17 Hemolysis induced by indicated treatment in whole human blood at a fixed concentration (A) or with increasing concentrations (B), and is expressed as percent whole blood hemoglobin content. Mean ± SD, n = 3. Photomicrographs demonstrate the absence of detrimental effect of Sr compounds on RBC morphology compared to untreated control (C).

5.4 Conclusions

The present work states that the substitution of SrO for SiO_2 has a major advantage over CaO. The density of the glasses increased with increasing concentration of SrO for SiO_2 while the network connectivity decreased in glass. It has shown significant effect on bioactivity, cytocompatibility and mechanical behavior. All the bioactive glasses exhibited HCA layer formation on their surfaces in the presence of SBF as confirmed by XRD, SEM and EDS. Whereas, the low NCB glasses have shown a significant enhancement in HCA crystallinity as compared to that of SrO substituted for CaO in reference bioactive glass. The elastic moduli of the bioactive glasses have increased significantly as the concentration of strontia increased for silica. The cell culture studies in the presence of low NCB glasses were found to exhibit better cell compatibility, significant cell growth and enhanced human blood compatibility as compared to reference glass. Thus, it is expected that these bioactive glasses are potentially applicable to clinical trials in bone regeneration and tissue engineering.